Identification of Central and Stretch Reflex Contributions to Human Postural Control

Pouya Amiri and Robert E. Kearney, *Life Fellow, IEEE*

***Abstract*— Human postural control requires continuous modulation of ankle torque to stabilize the upright stance. The torque is generated by two components: active contributions, due to central control and stretch reflex, and passive mechanisms, due to joint intrinsic stiffness. Identifying the contribution of each component is difficult, since their effects appear together, and standing is controlled in closed-loop. This article presents a novel multiple-input, single-output method to identify central and stretch reflex contributions to human postural control. The model uses ankle muscle EMGs as inputs and requires no kinematic data. Application of the method to data from nine subjects during standing while subjected to perturbations of ankle position demonstrated that active torque accounted for 84.0 ± 5.5% of the ankle torque. The ankle plantar-flexors collectively produced the largest portion of the active torque through central control, with large inter-subject variability in the relative contributions of the individual muscles. In addition, reflex contribution of the plantar-flexors was substantial in half of the subjects, showing its potentially important functional role; finally, intrinsic contributions, estimated as the residual of the model, contributed to 15% of the torque. This study introduces a new method to quantify the contributions of the central and stretch reflex pathways to postural control; the method also provides an estimate of noisy intrinsic torque with significantly increased signal to noise ratio, suitable for identification of intrinsic stiffness in standing. The method can be used in different experimental conditions and requires minimal a-priori assumption regarding the role of different pathways in postural control.**

***Index Terms*— Ankle, balance control, box-jenkins, closed-loop identification, EMG-driven model, EMG-torque, intrinsic stiffness, postural control, reflex stiffness, standing, stretch reflex, system identification.**

I. Introduction

DURING standing, the human body resembles an unstable inverted pendulum, subject to internal and external perturbations. The ankle muscles generate corrective forces that resist these perturbations and allow humans to keep their balance easily. These stabilizing forces are generated by three mechanisms: 1) Central activation of muscles, in response to visual, vestibular, and somatosensory feedback; 2) Stretch reflex activation of muscles, generated by peripheral mechanisms; and 3) ankle intrinsic stiffness, the joint mechanical resistance to the movement, generated by the visco-elastic properties of muscles, connective tissues, and inertial properties of the limbs [1]. Quantifying the contribution of each mechanism is essential to understand healthy and impaired postural control, and subsequently, develop interventions to address postural control problems [2]. However, such quantification is difficult, because these mechanisms act simultaneously, while only their overall result, such as body kinematics, ankle torque, and muscle electromyograms (EMG) can be recorded.

The ankle active torque, generated by neural activation, is the sum of central and stretch reflex components. EMG provides an indirect measure of neural activation and so can be used to estimate the active torque. If this is done, the intrinsic torque would be part of the residual once the active torque is removed from the total ankle torque.

Several studies have used EMG to study human postural control [3]–[6]. These have generally examined the EMG response to external perturbations to identify the central controller in standing. However, they did not quantify the functional contribution of central mechanisms in terms of the torque generated. Moreover, some of these studies used the EMG from only one muscle [4], [5], ignoring the role of the other muscles, while others assumed that all ankle muscles have the same activation dynamics [3], [6], which may have biased their estimates of EMG-torque relations.

The role of the stretch reflex in human postural control has been generally investigated by examining the stretch reflex EMG, evoked by imposed rotation of ankle joint or electrical stimulation of the tibial nerve [7], [8]. However, during functional situations, the stretch reflex EMG provides limited information about the mechanical contribution of the reflex mechanism, since the relation between EMG and torque is complex and nonlinear [9]. Therefore, it is essential to develop methods that quantify the mechanical contribution of stretch reflexes to postural control.

This study presents a novel method to obtain quantitative measures of central and stretch reflex torques in human postural control. A multiple-input, single-output (MISO), closed-loop, Box-Jenkins identification method was developed to decompose the ankle torque into its central and stretch reflex components, using EMG from the major ankle muscles. This provides a direct estimate of the mechanical contributions of

Manuscript received August 31, 2020; revised January 10, 2021; accepted January 30, 2021. Date of publication February 8, 2021; date of current version March 2, 2021. This work was supported by the Qatar National Research Fund (a member of Qatar Foundation) National Priorities Research Program under Grant 6-463-2-189; in part by the Canadian Institutes of Health Research under Grant MOP-81280; and in part by a fellowship from the Lloyd Carr-Harris Foundation. *(Corresponding author: Pouya Amiri.)*

Pouya Amiri is with the Faculty of Engineering, Imperial College London, London SW7 2BU, U.K. (e-mail: p.amiri@imperial.ac.uk).

Robert E. Kearney is with the Department of Biomedical Engineering, McGill University, Montreal, QC H3A 0G4, Canada.

Digital Object Identifier 10.1109/TNSRE.2021.3057785

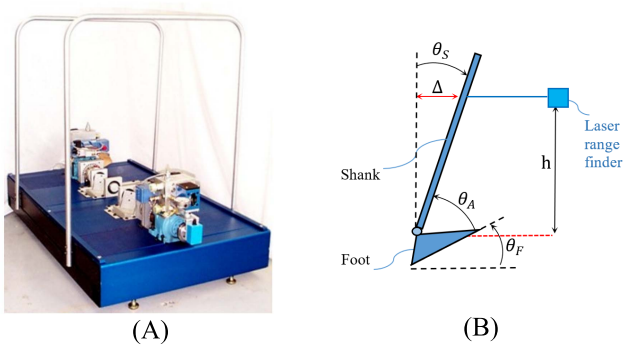

Fig. 1. (A) Experimental apparatus, (B) The shank angle (θ_S) was estimated by measuring its linear displacement (Δ) and dividing it by the range finder height, *h*, above the ankle axis of rotation; foot angle (θ_F) was measured by the actuator potentiometer; ankle angle (θ_A) was obtained using (1).

the central and reflex pathways to standing. The method also generates a noisy estimate of the intrinsic torque through its residuals.

The paper is structured as follows: Section II provides details of the experimental procedures, our model of balance control, and the identification methods. Section III presents the results, and Section IV discusses the findings.

II. Methods

A. Subjects

Nine subjects (6 males), aged 18–40 years, with no history of neuromuscular disease were examined. Subjects gave written consent to the experiments, which had been approved by McGill University's Research Ethics board.

B. Standing Apparatus

Fig. 1 shows the apparatus, comprising two pedals, driven by servo controlled electro-hydraulic rotary actuators (Rotac 26R-2 1V), able to apply independent bilateral position perturbations to the ankles of a standing subject. Each pedal had four load cells (The Omega™ LC302-100), which measured the vertical forces; these were used to calculate the ankle torque and the position of center of pressure (COP) relative to the ankle axis of rotation [10], [11].

High performance rotary potentiometers (Maurey Instruments 112-P19) measured each foot angle (θ_F, counter clockwise: positive), the pedal angle with respect to the horizontal (Fig. 1B). To determine shank angle (θ_S, counter clockwise: positive) with respect to the vertical (Fig. 1B), the linear displacement of a point on the shank was measured using a high performance laser range finder (1302-100, Micro-epsilon); this was converted to the angle, providing an angular resolution close to 0.01 degree (1.8×10^{-4} rad) [12].

As Fig. 1B illustrates, the ankle angle (θ_A) was computed as:

$$\theta_A = \pi/2 - (\theta_F - \theta_S) \tag{1}$$

By convention, dorsiflexing torques were taken as positive; ankle angle was $\pi/2$ when foot and shank were perpendicular. Consequently, angles less than $\pi/2$ corresponded to dorsiflexion and larger angles to plantarflexion.

C. EMG Recording

Surface EMG activity from the four major muscles about the ankle joint were measured. These included: Tibialis Anterior (TA), and the three muscles comprising the triceps surae (TS): medial and lateral gastrocnemius (MG and LG), and soleus (SOL). Single differential Delsys electrodes were applied, with an inter-electrode distance of 1 cm at the locations suggested by the Seniam project [13]. Electrode locations were verified by having the subjects perform manual resistance tests, while observing the EMG waveform on an oscilloscope to ensure a high signal-to-noise ratio and minimal cross talk. EMG signals were amplified, using a Bagnoli amplifier with an overall gain of 1000 and band-pass filtered between 20–2000 Hz.

D. Data Acquisition

To prevent aliasing, all signals were filtered at 486.3 Hz and then sampled at 1 KHz using 24 bit/8 channel, simultaneous-sampling, signal acquisition card (NI 4772, National Instrument). All subsequent analysis was performed using MATLAB. All sampled signals were digitally low pass filtered with a zero-phase-shift 6^{th}-order Chebyshev Type I filter with a cut-off frequency of 40 Hz and passband ripple of 0.05 dB and then down-sampled to 100 Hz.

E. Experiments

Participants were instructed to stand comfortably on the apparatus (looking forward, with their hands at their sides with no extra movement), and to maintain their balance when the random perturbations were being applied; mean foot angle was set to 0 degree. The actuators applied uncorrelated position perturbations to both ankles simultaneously. Perturbations were pseudo random binary sequences (PRBS), where pedal position switched between two values $(-0.01, 0.01$ rad) at random multiples of 200 ms (see Fig. 4A). PRBS inputs have a wide bandwidth, are unpredictable, and provide the greatest input power for a given amplitude [1], [14]. The perturbation switching interval and amplitude were selected to keep the perturbation mean absolute velocity low enough to avoid suppressing reflex responses [15], and to minimize postural disturbances [10]. Two trials, each lasting for two-minutes, and with different PRBS realizations were acquired for each subject. Trials were separated by at least two minutes of rest to prevent fatigue.

F. Human Postural Control Model

Fig. 2 is a block diagram of human postural control, considered in this study. The human body acts as an unstable inverted pendulum that must be stabilized in the presence of internal (e.g. respiration) and external disturbances, and destabilizing gravity torque. Stabilizing torques, generated in the ankle muscles, have three components:

1) Intrinsic torque (tq_I): due to ankle intrinsic stiffness, which acts as soon as there is a change in the joint angle.
2) Active torque (tq_A): due to neural activation of muscles, mediated by two feedback mechanisms:

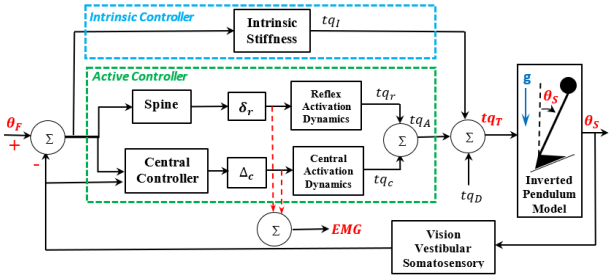

Fig. 2. Postural control model: the body is modelled as an inverted pendulum, subject to destabilizing gravity torque (g) and disturbances (tq_D). Corrective muscle torques are generated by a central controller (tq_c), stretch reflexes (tq_r), and intrinsic mechanical stiffness (tq_I) to achieve stable upright posture. The stretch reflex and central activations are measured by muscle EMG. The red signals are measurable, while the black signals are not.

A- Stretch reflex torque (tq_r): generated by phasic activation of TS muscles, due to spinal stretch reflex mechanism, acting with a short delay (δ_r) of about 40 ms [14].

B- Central torque (tq_c): generated due to a central response to the information about body position and orientation. The central torque is usually assumed to act with a lumped neural delay (Δ_c) of 100–200 ms [16].

It is difficult to determine the contribution of each component, since only the total ankle torque (tq_T) can be measured, which is:

$$tq_T(k) = tq_A(k) + tq_I(k) + tq_D(k) + n_m(k) \tag{2}$$

where k is time, and tq_D is the internal disturbance torque, and n_m is measurement noise. The total ankle torque can be considered as comprising an active torque ($tq_r + tq_c$), resulting from neural input, which can be estimated from EMG input [17]–[20], and residual torques (not generated directly by muscle activation), composed of intrinsic and disturbance torques plus measurement noise. Therefore, if EMG is used to estimate the active torque, we can subtract the active torque from the total torque to obtain a noisy estimate of the intrinsic torque.

The total active torque can be estimated as the sum of the active torques, generated by major muscles about the ankle:

$$tq_A(k) = \sum_{i=1}^{4} r_i\left(\underline{\theta}(k)\right) f_i\left(\underline{\theta}(k), \dot{\underline{\theta}}(k), a_i(k)\right) \tag{3}$$

where r_i and f_i are the moment arm and active force of muscle i (i can be MG, LG, SOL, and TA). a_i is the muscle activation, and $\underline{\theta}$ and $\dot{\underline{\theta}}$ are joint angle and velocity. We recently showed that ankle joint position changes were small during our experiments (peak-to-peak amplitude <0.08 rad$\sim$ 4°) [10], [21]. Consequently, we assumed that the ankle angle is constant. We also assumed that the EMG-torque relation is not explicitly velocity dependent for our perturbations (the relation might vary if the perturbation properties changed or if there were large rapid postural movements). These assumptions simplify (3), so that muscle forces change with activation only and moment arms are constant. In addition, we assume that muscle forces can be predicted from EMG, using a low-pass linear transfer function (TF) [19]. Therefore, (3) becomes:

$$tq_A(k) = \sum_{i=1}^{4} r_i H_i(q)\, e_i(k) \tag{4}$$

where q is the shift operator, H_i and e_i are the TF and EMG of the i^{th} muscle. We will make the following additional assumptions:

1) The EMG-force TFs for TS muscles are different for central and reflex mechanisms and must be modelled separately.
2) The EMG-force TF of the three TS muscles have the same dynamics (poles and zeros) but different gains.
3) The torque produced by TS can be predicted from the weighted sum of the EMGs of the three muscles as in [3], [6], where optimal weights must be determined.
4) Close examination of the EMG activity of TA muscle showed that there was no burst of reflex activity associated with plantar-flexing pulses as is evident in Fig. 4. Therefore, we did not include a contribution from TA reflex activity.

These assumptions, transform (4) to a multiple-input, single-output (MISO) linear model:

$$tq_A(k) = H^c_{TS}(q)\, e^c_{TS}(k) + H^r_{TS}(q)\, e^r_{TS}(k) + H^c_{TA}(q)\, e^c_{TA}(k) \tag{5}$$

where H^c_{TS}, H^r_{TS}, and H^c_{TA} are the TFs from central TS input [1] (e^c_{TS}), reflex TS input (e^r_{TS}), and central TA input (e^c_{TA}) to torque. The central and reflex TS inputs are given by:

$$\begin{aligned} e^c_{TS}(k) &= w^c_1 EMG^c_{sol}(k) + w^c_2 EMG^c_{MG}(k) + w^c_3 EMG^c_{LG}(k) \\ e^r_{TS}(k) &= w^r_1 EMG^r_{sol}(k) + w^r_2 EMG^r_{MG}(k) + w^r_3 EMG^r_{LG}(k) \end{aligned} \tag{6}$$

where w^c_j and w^r_j are the weights of the TS muscles and e^c_{TA} is simply the TA EMG. The EMGs in (6) were obtained in three steps: 1) the recorded EMGs were full wave rectified. 2) Each EMG was normalized to the root mean square (RMS) of its postural activity; the postural activity of each muscle was estimated by replacing the EMG activity during stretch reflex period (which started at the peak velocity of dorsi-flexing pulses and lasted for 80 ms) with the EMG activity observed for the 80 ms prior to the reflex. This ensured that the postural activity due to sway was not biased by the large reflex activities [10]. 3) EMGs were decomposed to their reflex and central component as described next.

G. EMG Decomposition

We noted that central activation of TS muscles varied continuously with postural sway. In contrast, reflex activity period started at the peak velocity of dorsi-flexing pulse perturbations, reached a maximum 40 ms afterwards, and lasted for a total of 80 ms (The two-sided filter used to filter the data (section II.D) was symmetric about zero-lag and consequently

[1] For the inputs, the superscripts c and r show central and reflex, respectively, and the subscripts show the muscles (TS, LG, MG, SOL, TA).

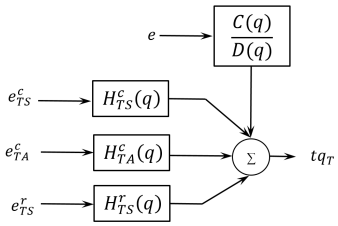

Fig. 3. MISO Box-Jenkins structure for central and reflex EMG-torque relationships.

did not change the timing of the reflex activity with respect to the peak velocity of the dorsiflexing pulse) [10]. Therefore, to estimate the central EMG activity, we: (1) identified the peak velocities of dorsi-flexing pulses, and (2) estimated the central EMG during reflex response by replacing EMG samples in reflex period with randomly permuted EMG samples from the 80 ms preceding the reflex period (assuming the amplitude structure of central EMG during reflex period was the same as the short preceding period) [6]. The reflex EMG was then estimated by subtracting the estimated central EMG from the total EMG. The cross correlation between the stretch reflex and central components (generated by our decomposition method) was small for lags shorter than the expected difference in conduction delays between the reflex and central pathways.

H. Identification

In standing, sensory signals from body movements are used to generate stabilizing muscle forces, which in turn generate body movements, sensed by sensory systems. Consequently, the EMG and torques are recorded within a closed-loop (Fig. 2). In such conditions, specialized identification methods are required to obtain unbiased estimates of the relation between EMG and ankle torque. The prediction error method (PEM), in which the system and noise are modelled parametrically, is one such method [22]. It will give unbiased estimates from closed-loop data with an arbitrary feedback, provided the model parameterizations are flexible enough. To achieve this, we used the MISO Box-Jenkins structure illustrated in Fig. 3; this models the system and noise dynamics independently as:

$$tq_T(k) = H^c_{TS}(q)\, e^c_{TS}(k) + H^r_{TS}(q)\, e^r_{TS}(k) + H^c_{TA}(q)\, e^c_{TA}(k) + \frac{C(q)}{D(q)} e(k) \quad (7)$$

where $e(t)$ is an unknown white random sequence. The transfer function $C(q)/D(q)$ models the intrinsic torque, internal disturbances, and measurement noise.

The weights in (6), and the poles and zeros in (7) are unknown and must be identified. These were estimated in three steps, using the data from the first trial:

1) Identification of TS EMG Weights: To determine the weights in (6), we examined a wide range of structures (i.e. the number of poles and zeros) for the TFs in (7). For each structure, we used nonlinear optimization to find the weights that minimized the RMS error between the measured torque and the model prediction. The optimization comprised an outer loop and inner loop: The outer loop selected a set of weights in (6) and passed them to the inner loop, which determined the TF parameters that minimized the RMS torque error for the specified set of weights. The inner loop optimization was performed using MATLAB's Identification Toolbox. The outer loop optimization was done using MATLAB's fmincon gradient descent search; fmincon was run with five random initial conditions and the weights giving the lowest RMS error were selected.

The approach demonstrated that a Box-Jenkins structure with 3 zeros and 3 poles for the EMG-torque TFs and with 10 zeros and 25 poles for the noise model, provided good torque prediction for all subjects. This model structure may have been over-parameterized, but it provided good prediction accuracy and therefore, was effective to find the optimal weights for the EMG inputs in (6).

2) Identification of EMG-Torque Transfer Functions: This step refined the estimates of structures and parameters of the EMG-torque and noise TFs, using the weights determined in step 1. Doing so required selecting the number of poles and zeros for each TF *a-priori*. Previous studies of postural control assumed that the EMG-torque relationship was a 2nd order low-pass TF [3, 5]. However, in our pilot studies we found that more complex structures could be required. Therefore, to determine the optimum structure, we estimated the parameters for all combinations of 1) EMG-torque TFs having 2 or 3 poles, and the number of zeros ranging from 0 to the number of poles (Models with more than three poles or zeros did not improve model performance); and 2) Noise TFs with 0-10 zeros and 5-25 poles (to ensure that the noise model was flexible enough to deliver unbiased estimates of the dynamics). This resulted in a total of 118,041 possible model structures. We selected the "best model" based on the following criteria:

a) Percentage variance accounted for (%VAF):

$$\%VAF(M) = 100\left(1 - \frac{\sum_{k=1}^{N}\left(tq_T(k) - t\hat{q}_A(k,M)\right)^2}{\sum_{k=1}^{N} tq_T^2(k)}\right) \quad (8)$$

b) Minimum description length (MDL):

$$MDL(M) = \left(1 + \frac{M log(N)}{N}\right)\sum_{k=1}^{N}\left(tq_T(k) - t\hat{q}_A(k,M)\right)^2 \quad (9)$$

c) Akaike Information Criterion (AIC):

$$AIC(M) = Nlog\left(2\pi \sum_{k=1}^{N}\left(tq_T(k) - t\hat{q}_A(k,M)\right)^2\right) + 2M + N \quad (10)$$

where M is the number of model parameters, $N = 12000$ is the number of samples (after decimation), and $t\hat{q}_A$ is the total predicted active torque. The %VAF picks the model with the best fit, irrespective of the number of parameters. The MDL and AIC account for both the fit and model complexity. It is felt that MDL favors fewer parameters over the goodness of the fit, whereas AIC favors the latter.

To find the final model, we first determined a model based on each criterion. This was defined as the model with the best performance (i.e. highest %VAF or lowest MDL/AIC) that also met the following criteria:

1) All EMG-torque TFs were stable.

2) The residuals had a near white power spectrum and was not correlated with any of the inputs.

3) The frequency response function (FRF) and impulse response function (IRF) of EMG-torque models were low pass.

4) The noise model was stable (otherwise PEM would fail).

Then, the three candidate models (selected using VAF, MDL, AIC) were used to predict the torque from the second trial. The model with the highest VAF was selected as the final model; however, if the VAF difference among models were less than 1%, the model with fewest parameters was chosen.

In some cases, the TA or/and stretch reflex torques were so small that their dynamics could not be reliably estimated, due to the low signal to noise ratio. Such cases were readily recognized, since the estimated FRF and IRF for the TA or/and stretch reflex response did not have the expected low pass behavior and their torque predictions were small and noise-like. The resulting errors might bias the estimates of central TS EMG-torque dynamics. Therefore, in such cases, the identification procedure was repeated excluding the TA or/and stretch reflex dynamics.

3) Re-Identifying the Input Weights: In the final step, we fixed the parameters and structure of the optimal TFs, obtained in step 2, and re-estimated the EMG weights in (6) using MATLAB's fmincon function, to minimize the RMS error between the measured torque and the model prediction. This generated the final model.

I. Conversion to Continuous Time

The identification procedure was done using sampled data and so yielded discrete-time TFs. To make interpretation more straightforward, the discrete-time models were transformed to their continuous-time equivalents, using the inverse of the bilinear transform. Thus, the shift operator was replaced by:

$$q = (2 + st_s)/(2 - st_s) \tag{11}$$

where t_s is the sampling interval (0.01 s after decimation) and s is the Laplace operator. The continuous-time TFs had high frequency poles and zeros, whose contributions were beyond the system bandwidth. We identified such extraneous poles and zeros by comparing the FRFs and simulated outputs of models with/without these poles and zeros. Any continuous pole or zero, which had no significant effect on the simulated output was discarded (i.e. if the change in %VAF was less than 1%). The FRF of the final TFs were determined by substituting $s = j\omega$ for the frequency range $\omega = 0.1 - 50$Hz.

III. Results

A. Experimental Data

Fig. 4 shows 15 seconds of a typical trial (for S1L[2]). Fig. 4A shows the foot angle, which switches rapidly between two positions, in a PRBS waveform, with a peak-to-peak amplitude of 0.02 rad. Fig. 4B shows the shank angle, with low frequency movements associated with sway. Fig. 4C shows that the ankle angle changed less than 0.08 rad ($< 4.6°$), verifying the assumption of small joint movement, used to simplify (3).

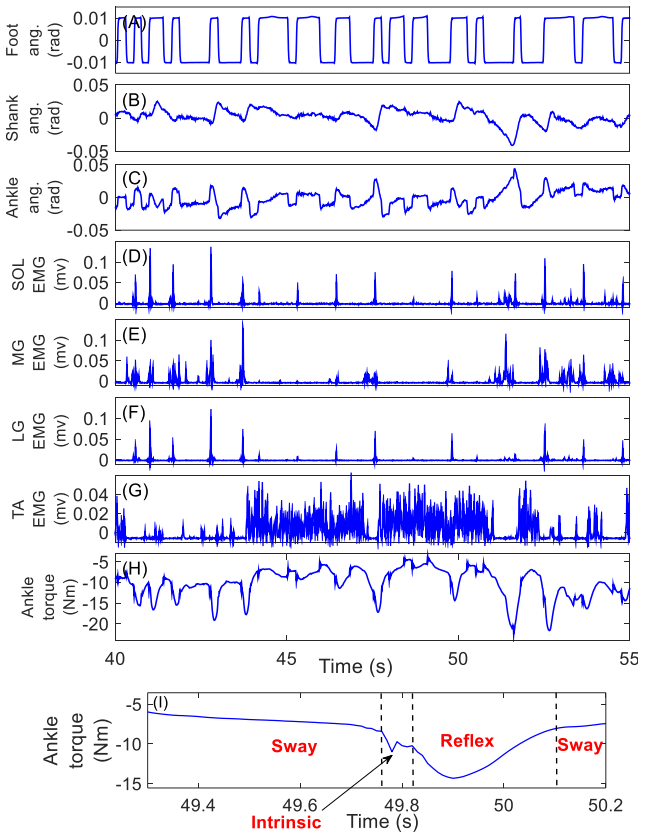

Fig. 4. Sample experimental data; (A) foot angle, (B) shank angle, (C) ankle angle, (D) SOL EMG, (E) MG EMG, (F) LG EMG, (G) TA EMG, (H) ankle torque, (I) ankle torque (S1L).

Fig. 4D&E&F illustrate the two components present in the SOL, MG, and LG EMGs. These were: (i) phasic peaks of activity, following dorsi-flexing foot perturbations due to reflex activity; and (ii) periods of smaller, less synchronous baseline activity at various times (e.g. between 50 to 55 s). The TA EMG (Fig. 4G) displayed large, asynchronous activity during some intervals – usually when there was little TS EMG activity. Fig. 4H shows the ankle torque; three torque components are evident, as illustrated on an expanded time scale in Fig. 4I: (i) low-frequency modulation of the torque with body sway; (ii) short rapid oscillatory intrinsic responses during pulse perturbations, and (iii) large downward peaks, associated with stretch reflex EMGs.

B. EMG Decomposition

Fig. 5B-D illustrates the result of decomposing TS EMGs into its central and stretch reflex components, as described in II.G. For all TS muscles, the reflex component was non-zero only for 80 ms-intervals after the peak velocity of dorsi-flexing pulses, while central activity could occur at any time.

[2]Sip stands for side p (L= Left, R=Right) of subject i (i = 1, . . . , 9).

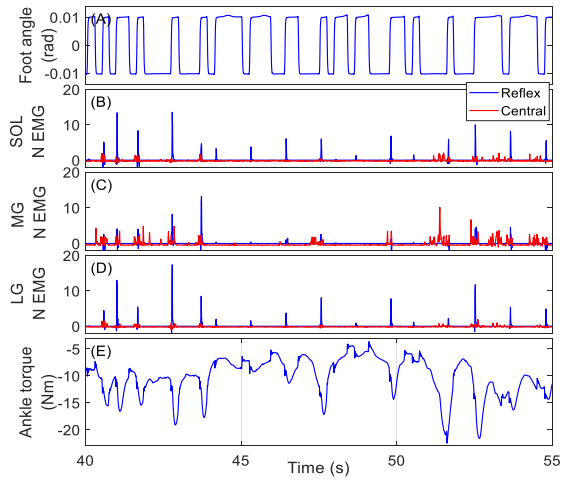

Fig. 5. Decomposition of TS normalized EMG (N EMG) to central and reflex components for S1L's signals in Fig. 4; (A) foot angle, (B) SOL, (C) MG, and (D) LG normalized EMG, (E) ankle torque. The estimated reflex EMG is shown in blue and the estimated central EMG is shown in red.

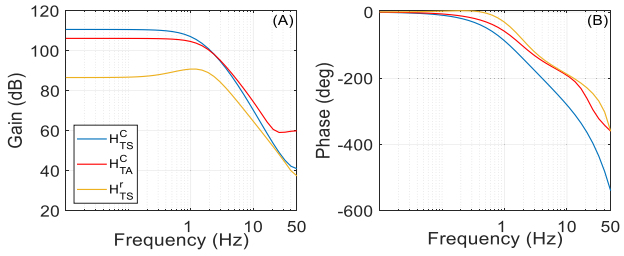

Fig. 6. FR of the identified TFs for S1L, (A) Gain, (B) Phase.

The reflex activity of SOL and LG was substantially larger than their central activity. Therefore, removing the estimated central component from the total EMG always generated reflex EMGs with large, positive components (Fig. 5B&D). However, for MG, the central and stretch reflex amplitudes were comparable in size. As a result, subtracting the central component from its total EMG sometimes resulted in reflex components with zero or negative amplitudes. In such cases, only SOL and LG reflex components were used in (6) to estimate the reflex TS input. Although, this happened in most cases, we believe removing the MG reflex EMG from the total reflex input did not affect the reflex torque estimation, because the MG contribution to reflex torque was captured by LG and SOL reflex EMG, due to high degree of synchronization and correlation between the reflex activity of the three TS muscles.

C. Typical Identification Results

Fig. 6 shows the results of applying the identification to the data from Fig. 4(60 seconds is shown). The three input signals are the central TS input (e^c_{TS}, Fig. 6B), central TA input (e^c_{TA}, Fig. 6C), and the reflex TS input (e^r_{TS}, Fig. 6D). The TS and TA central input signals were intermittently active; generally, when one was active, the other was silent. Fig. 6D shows the reflex TS input, comprising bursts, starting 40ms after dorsiflexing pulses and lasting for 80 ms.

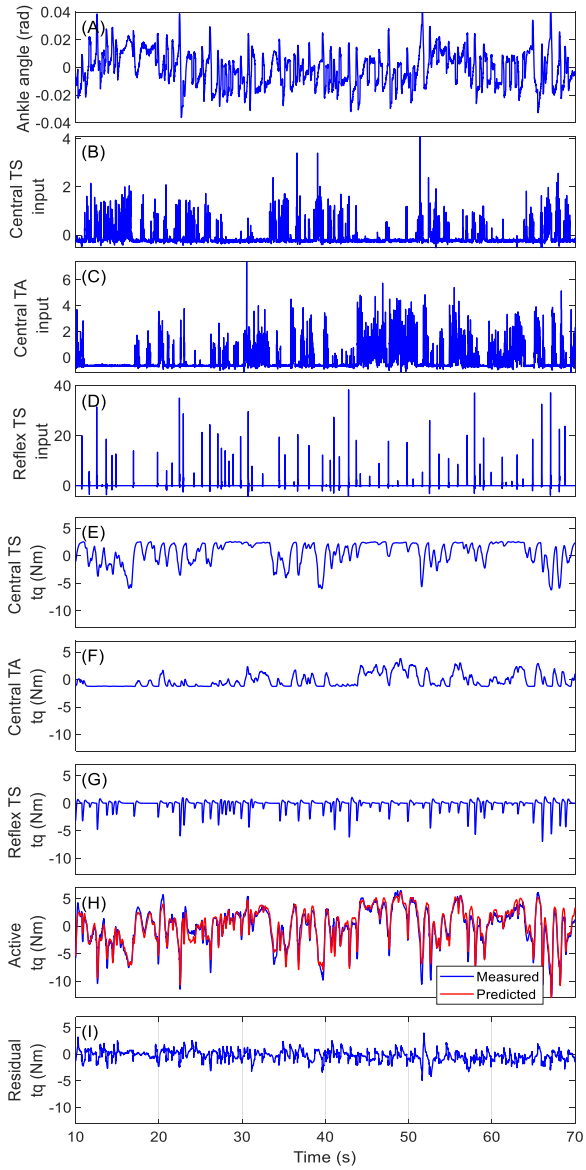

Fig. 7. Typical identification results (A) ankle angle, (B) central TS input, (C) central TA input, (D) reflex TS input, (E) predicted central TS torque, (F) predicted TA torque, (G) predicted reflex TS torque, (H) measured torque (blue) and total predicted active torque (red), and (I) residual torque (S1L) (The means of EMG inputs and ankle torque were removed for the identification and prediction).

Fig. 6 also shows the active torque components, predicted by the identified model. The central TS torque (tq^c_{TS}, Fig. 6E), was largest, while the central TA (tq^c_{TA}, Fig. 6F) and the reflex TS (tq^r_{TS}, Fig. 6G) torques were smaller, but still substantial (peak-to-peak amplitudes were 8.8 Nm for tq^c_{TS}, 5.0 Nm for tq^c_{TA}, and 7.9 Nm for tq^r_{TS}). The non-zero baseline torques in Fig. 6E&F are due to removal of the mean from central TS and TA inputs in Fig. 6B&C, which was necessary for the identification.

Fig. 6H shows the total predicted active torque, in red, superimposed on the measured torque in blue. The two torques were very similar and the predicted active torque accounted for 92.8% of the measured torque variance.

Fig. 6I shows the residual torque, ($C(q)/D(q)e(t)$ in (7)), which accounted for 7.2% of the torque variance. The residual

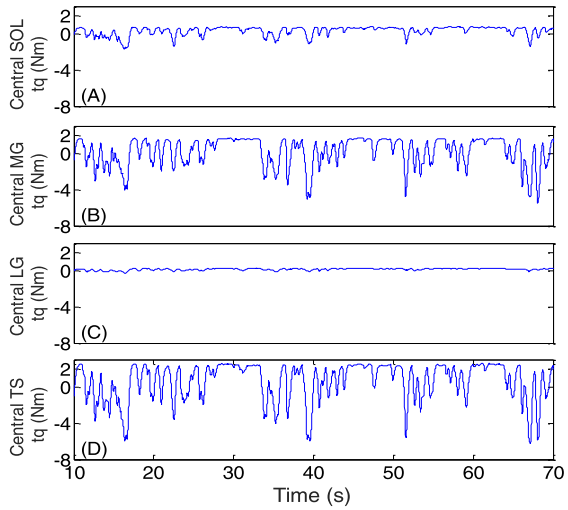

Fig. 8. Break down of torques from Fig. 6 (A) central SOL torque, (B) central MG torque, (C) central LG torque, and (D) central TS torque (S1L).

comprised the intrinsic torque, internal disturbances, and measurement noise.

Fig. 7 shows the breakdown of the TS central torque from Fig. 2. MG, SOL, and LG torques accounted for 55.4%, 16.0%, and 3.3% of the total torque, respectively. It is evident that the three TS muscles were active synergistically and had similar trends. Nonetheless, all three EMGS contributed to the central TS torque and removing any of the EMG signals resulted in a substantial reduction (>3%) in the overall %VAF.

Fig. 8 shows the FRFs of the estimated EMG-torque TFs. These were low pass in nature, with corner frequencies of 1.1 Hz, 1.4 Hz, and 3.1 Hz for H^c_{TS}, H^c_{TA}, and H^r_{TS}. Moreover, the phases started at 0° for all TFs and then decreased at higher frequencies based on the number of the poles and zeros.

D. Identification Results for All Subjects

Table I shows the number of poles for the continuous TFs, their bandwidth, and %VAF of both the identification and cross-validation trials for the predicted active torques of all subjects (The experimental data and the identified models presented were obtained using the first experimental trial for each subject. The second trial was used only for the final model selection and cross-validation of the models' predictive performance). In all case, there were no significant continuous zeros. Note that the data for S6R was discarded, since it was corrupted by a large, low frequency noise of unknown origin. In all cases, the active torque predicted by the identified models accounted for most of the observed torque; the %VAF was 84.0 ± 5.5% (mean ± standard deviation) with min = 72.0%, and max = 92.8%. As expected, the %VAF of the cross-validation trial was usually slightly smaller than for the identification trial (although in 3 cases, it was higher, Table I); the median difference in %VAF across all cases was 3.0%.

TABLE I
IDENTIFICATION RESULTS FOR ALL SUBJECTS; S STANDS FOR SUBJECT; L AND R SHOW LEFT AND RIGHT ANKLES. P, Z, AND BW SHOW THE NUMBER OF POLES, ZEROS AND BANDWIDTHS OF THE IDENTIFIED TFS. % VAF IS FOR THE TOTAL ACTIVE TORQUE AND IS PRESENTED FOR THE IDENTIFICATION (ID) AND CROSS VALIDATION (CV) TRIAL

S		H^c_{TS}		H^c_{TA}		H^r_{TS}		$\frac{C(q)}{D(q)}$		%VAF	
		p	BW (Hz)	p	BW (Hz)	p	BW (Hz)	z	p	ID trial	CV trial
1	L	3	0.9	2	1.4	3	3.1	1	10	92.8	93.2
	R	2	1.2	3	0.5	2	2.5	2	6	85.2	82.2
2	L	3	0.4	-	-	2	1.5	1	14	81.7	79.1
	R	3	0.7	-	-	3	1.5	9	12	87.3	78.3
3	L	2	1.0	2	0.6	3	1.0	1	7	82.6	84.7
	R	3	0.6	2	2.7	2	2.7	0	15	86.1	75.7
4	L	3	0.6	-	-	2	1.9	6	13	89.8	82.5
	R	3	0.5	-	-	2	2.2	1	7	80.2	75.8
5	L	3	0.8	-	-	2	2.5	7	9	79.1	73.5
	R	2	0.7	-	-	3	2.3	8	9	79.2	77.8
6	L	2	1.0	-	-	3	2.8	3	7	80.5	77.2
7	L	2	0.5	-	-	2	2.1	3	5	78.7	76.1
	R	2	0.5	-	-	2	2.0	0	5	72.0	69.7
8	L	2	0.7	3	1.0	3	2.4	6	8	91.5	88.9
	R	2	0.9	2	1.0	2	1.7	6	10	88.0	82.6
9	L	3	0.3	-	-	2	1.1	8	13	84.8	86.2
	R	3	0.6	2	0.6	2	1.8	8	11	88.6	84.0

Table I also shows that the EMG-torque TF structures differed among the subjects (some having 2 poles and others 3), and even between the left and right legs of the same subject. The noise model structure also varied, with the number of zeros ranging from 0-9 and the number of poles from 5-15. In addition, the TA TF was reliably estimated in only 7/17 cases; the TA made no significant contribution to the torque in the other 10 cases.

All EMG-torque relations were low-pass in nature (similar to Fig. 8, but had different bandwidths. The bandwidth of the central TS EMG-torque dynamics, H^c_{TS}, was 0.7 ± 0.2 Hz, whereas that of the reflex TS EMG-torque dynamics, H^r_{TS}, was much higher, 2.1 ± 0.6 Hz. The bandwidth of the central TA EMG-torque dynamics, H^c_{TA}, was 1.0 ± 0.7 Hz. Moreover, the phase of all TFs for all subjects started at 0 and then decreased at higher frequencies, according to number of poles.

E. Reflex and Central Contributions

Fig. 9A compares the %VAF of the active and residual torques for all subjects. It is evident that active torque accounted for most of the total torque with a %VAF of 84.0±5.5%, while the %VAF of the residual was 16.3±4.2%. The sum of the %VAF of active and residual sometimes is somewhat larger than %100, because the residual contains intrinsic torque, which is not completely uncorrelated with the active torque [23].

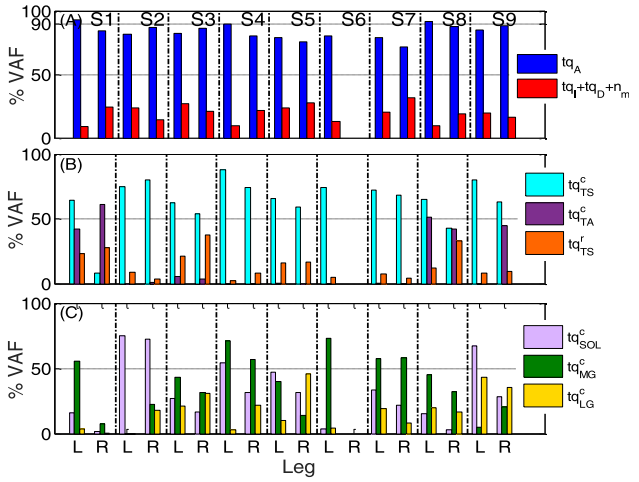

Fig. 9. %VAF of the predicted torque components; (A) %VAF of the total active (blue) and the residual (red) torques, (B) %VAF of the central TS (tq^c_{TS}, cayan), central TA (tq^c_{TA}, purple), and reflex TS (tq^r_{TS}, orange) torques; (C) %VAF of SOL (light purple), MG (green), and LG (yellow) central torques; L and R show left and right sides. Si ($i = 1, \ldots, 9$) shows subject i. Right side of S6 was discarded, due to an unknown noise presence.

Fig. 9B compares the contributions of the central and stretch reflex torques for all cases. The central TS torque (tq^c_{TS}) was the largest in all but one case with an average %VAF of 64.4± 18.0%. The central TA contribution was substantial in only 7/17 cases, with %VAFs ranging 3.3-61.1%. The reflex TS contribution (tq^r_{TS}) was always smaller than the central TS contribution, but it was very variable, with the %VAFs ranging from a low of 2.5% to a high of 37.6%.

Fig. 9C summarizes the central contributions of SOL, MG, and LG to the ankle torque. There was large inter-subject variability in the relative size of the contributions. Thus, MG (%VAF 5.1-73%) accounted for the greatest torque variation in 11/17 cases, SOL in 4/17 cases, and LG in only 2/17 cases.

F. Soleus Reflex and Central EMG-Torque Dynamics

Fig. 10A shows the bandwidth of SOL central and stretch reflex TFs of all cases (these were the same as bandwidth for H^c_{TS} and H^r_{TS}, as shown in Table I, since we assumed all TS muscles shared the same dynamics). It is evident that the reflex dynamics had a higher bandwidth than the central dynamics. The median reflex bandwidth was 2.0 Hz, while it was 0.6 Hz for the central dynamics.

Fig. 10B shows that the DC gain of central SOL TF were always larger than that of reflex SOL TF. The median DC gains were 113.8 and 104.1 dB for central and reflex TFs (Note that to obtain the final DC gains in Fig. 10B, the initial DC gain of the identified TFs, H^c_{TS} and H^r_{TS}, were multiplied by the weight of central and reflex SOL input in (6) to account for their contributions; then, to provide the relationship from *raw* central EMG and reflex SOL EMG to torque, the DC gains were multiplied by the normalization factors, used originally to form the input EMGs in (6), which was the RMS of postural activity of SOL and the same for both EMG^c_{sol} and EMG^r_{sol}).

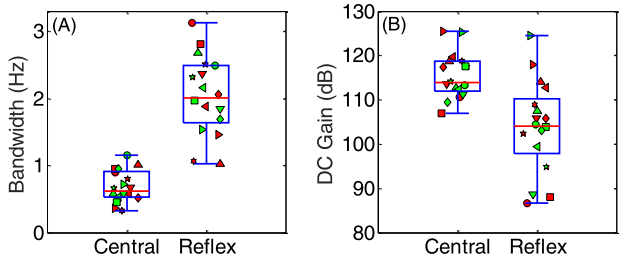

Fig. 10. Comparison of SOL central and stretch reflex bandwidth and DC gain; (A) bandwidth, and (B) DC gain. For the box and whisker plot, the horizontal lines show minimum, 25th percentile, median (red line), 75th percentile, and maximum (from bottom to top). The individual points show the values for the cases, whereas identical markers belong to the same case.

IV. Discussion

We developed a method to determine central and stretch reflex contributions to ankle torque in standing. The method uses EMGs from ankle muscles as inputs and requires no kinematic data. Applying this method to data acquired during normal standing led to the following main findings: 1- Active contributions to ankle torque were much larger than those from intrinsic stiffness and other noises (%VAF $= 84.0 \pm 5.5\%$ vs. $16.3 \pm 4.2\%$).2− The central torque was generated mostly by ankle plantar-flexor muscles ($64.4 \pm 18.0\%$). TA, the ankle dorsi-flexor, contributed to a minority of cases; only 7/17 cases had a %VAF$>3.3\%$. 3− Stretch reflex contributions were very variable, generating torques comparable to those of central (i.e. %VAF$>$ 15%) in 7/17 cases. 4− Reflex EMG-torque dynamics had a higher bandwidth but lower DC gain than central EMG-torque dynamics.

A. Identification Performance

Our method predicted that the active torques accounted for $84.0 \pm 5.5\%$ of the torque variance. This high %VAF and low cross-correlation between the inputs and the residual torques demonstrated that the model captured most of the system dynamics. The high %VAF also supports our assumption that ankle movements were small enough to allow a linear, time-invariant formulation. Moreover, visual inspection of the EMG-torque FRFs showed the low pass behavior, expected from previous studies [4], [18], [19]. Consequently, we believe this model described postural control dynamics well.

We believe that our EMG decomposition method, combined with the parametric identification using PEM, generated unbiased estimates of the EMG-torque TFs. The EMG decomposition method may have introduced some noise in our estimates of central and reflex EMGs (used in (6)). However, we used a separate flexible noise model, so that the PEM identification procedure is guaranteed to generate unbiased estimates of the dynamics in the presence of input noise.

The noise from the decomposition procedure could also increase the random error of our estimates. PEM minimizes the difference between the measured and predicted torque during the whole trial; however, the decomposition noise was present only during the short, 80-ms long intervals, following dorsi-flexing pulses. As a result, this noise was present in only

the short segments of the trial where reflexes were present (Each trial contained 114 ± 6 pulse perturbations, so that reflex activity was present for 9.1 ± 0.48 s or about 7.5% of the trial). Consequently, we believe that this noise would have minimal effect on the estimates of *central EMG-torque dynamics*. Furthermore, the reflex EMG amplitude was generally much larger than that of central EMG. Consequently, the noise added by the decomposition process is likely to have had only a small effect on the estimates of the *reflex EMG-torque dynamics*.

Parametric models can be criticized, because they require *a-priori* knowledge of the model structure. We addressed this drawback by identifying many model structures, selecting three candidate models according to three widely used model selection criteria, and choosing the final model using cross-validation. Therefore, our final parametric model structure was chosen to best fit our data and was not assumed *a-priori*.

A few studies of postural control have examined ankle EMG-torque dynamics in standing [4]–[6]. However, they estimated the closed-loop FRF of the postural control system and the performance of these models was not evaluated in terms of predicted torque. One study that did evaluate torque prediction reported %VAFs ranging 52-95% in four subjects [4]. These %VAF were obtained for the contribution from the sum of both intrinsic and active components, using MG EMG and kinematics as model inputs. Our model, used only the EMGs of the major ankle muscles, predicted only the active torque, and generated consistently higher %VAFs. This suggest that multiple EMGS are needed to accurately predict the active torque during standing.

Our results also showed that the subjects employed a variety of muscle recruitment strategies for postural control. Therefore, we believe that any model of postural control must include all the major ankle muscles. Previous studies used either EMG from a single muscle [4], [5], or in one case the weighted sum of all ankle muscles [3], [6]. The latter assumed that the EMG-torque dynamics of TS and TA muscles were the same. Our results showed the dynamics of ankle plantar-flexors and dorsi-flexors were quite different.

B. EMG-Torque Dynamics

We selected the structures of the parametric EMG-torque TFs objectively, using three performance criteria. We found that a discrete time TF with two or three poles with a variable number of zeros was needed. However, after conversion to continuous-time TFs, we found that the zeros were at high frequencies and so had little effect on the dynamic response. Rather, it was the poles that determined the dynamics of the continuous TFs. Therefore, we concluded that the continuous-time EMG-torque TFs were 2^{nd} or 3^{rd} order low-pass with no zeros. Previous studies of standing have assumed *a-priori* fixed 2^{nd} order structure for EMG-torque relation [3, 5, 6]. Our results clearly demonstrate that this assumption may lead to models that fit the data poorly; in one case, the %VAF of a 2-pole model was 25% lower than that of a 3-pole model.

The EMG-torque TF estimates were all low pass in nature; however, their gain and phase properties differed. We found that H^c_{TA}, H^c_{TS}, and H^r_{TS} had bandwidths equal to 1.0 ± 0.7 Hz, 0.7 ± 0.2 Hz, and 2.1 ± 0.6 Hz. Other studies reported similar values between 0.95 to 1.43 Hz [3], [5], [6]. Small differences exist, probably due to differences in modelling method [3], [5], [6], or discrepancy of the contraction bandwidth [19], depth of torque modulation [18], and ankle joint position [24].

C. Central and Reflex EMG-Torque Dynamics

Our results showed that the reflex TS EMG-torque dynamics had a higher bandwidth and lower DC gain than the central dynamics. Differences in motor-unit synchronization might explain such differences. Yao *et al.* showed that amplitude of the EMG, but not the muscle force, increased as motor-unit synchronization increased [25]. In our case, we would expect that the short latency stretch reflex responses would be more synchronized than the central response, since the latter is generated by multiple sensory pathways with different, long delays. Another possibility is that the stretch reflex recruits motor units in a manner similar to rapid muscle contractions, where large fast motor units (MU) are recruited at a lower than normal force threshold [26]. In contrast, the asynchronous central activation would recruit MUs in the normal order. Thus, stretch reflex activation would generate output forces with smaller gain, but higher bandwidth.

Consistent with our results, Toft *et al.* showed that the EMG-torque DC gain was lower for stretch reflex than voluntary contractions [27], and Genadry *et al.* and Sinkjaer *et al.* showed that increasing the rate of muscle force development resulted in higher bandwidth EMG-torque dynamics [17], [18].

D. Central and Reflex Contributions to Ankle Torque

Our results demonstrated that active mechanisms contributed more than other components to the ankle torque. Active torque accounted for an average 85% of the total torque, whereas the residual, which provided an estimate of noisy intrinsic torque, explained the rest of the measured torque.

Intrinsic stiffness is difficult to estimate in standing due to its small contribution [3], [6], [16], [28]. Some studies estimated the intrinsic stiffness from the response to transient perturbations in standing, reporting normalized stiffness values from 15% to 91% [10], [29]. However, these values do not quantify the intrinsic torque, which depends on both stiffness and joint movement. Only one study reported the intrinsic mechanisms contributed to 26% of total torque [4].

Our results demonstrate that the muscle recruitment strategy varied among subjects. In most cases, the central TS contribution to the total torque was highest, where MG generated the largest component, while SOL and LG contributions were substantial. TA was generally silent, but in some individuals, it contributed significantly to the torque, sometimes even higher than TS muscles (e.g. S1R, Fig. 9C).

Individual muscle contributions to postural control have been rarely quantified. Several studies used either EMG from

only one muscle [4], [5] or multiple muscles with no indication of individual muscles contribution to the torque [3], [6]. Kiemel *et al.* did show that medial gastrocnemius muscle generated the highest coherence with perturbations [3], which is consistent with our results. This can be also seen in Fig. 4, where MG shows largest activations modulation (compared to SOL and LG) consistent with the body sway. In addition, similar to our results, TA was reported to be mostly silent and sometimes active, with small contributions in most cases [3]–[5].

Our results showed that the stretch reflex contribution to control was variable among the subjects, substantial in some cases. It was previously shown that stretch reflex could contribute significantly to the ankle torque in supine conditions [9], [14]; however, this is the first study to quantify the mechanical contribution of the stretch reflex to postural control. This is important, because the stretch reflex has been investigated by examining EMG amplitude of the TS muscles [7], [8]. However, this may be misleading, as it was reported both in supine [14] and standing [30] conditions that the stretch reflex EMG and torque may show different trends [9].

The findings of the current study hold for normal standing; it is expected that the contributions of different pathways change substantially with altered postural operating conditions; for example, intrinsic contributions are much higher during forward lean [31].

E. Strengths and Limitations

Our method utilizes EMGs from the major ankle muscles to determine the TF and mechanical contributions of central and stretch reflex pathways to postural control. It has some important strengths: 1) It does not require measures of kinematics and so is straightforward to apply using only EMG and force plate measurements. 2) It estimates the intrinsic torque with much improved signal to noise ratio, making it possible to estimate the intrinsic stiffness reliability. 3) It generates simple models for muscles with minimal a-priori assumptions. 4) It can be easily applied to different postural operating conditions and/or different types of perturbations, provided that the perturbation properties and resulting joint angles are stationary.

There are some limitations associated with our method. We used perturbations with small amplitudes (0.02 rad or 1.15 deg) to ensure minimal disturbance to the postural control mechanism. This allowed us to use linear time invariant models for muscles active torques. We expect that the method will work with other perturbation amplitudes, provided the properties are stationary; while the estimated models might be different, the torque predictions should still work. For perturbations or experimental protocols that result in non-stationary conditions (e.g. large perturbation amplitudes), time-varying and/or nonlinear methods would be necessary.

Moreover, from a physiological point of view, we would expect that larger body sway (as a result of larger perturbations or different experimental conditions) to modulate the control strategy: central contributions will still account for the largest variability of torque, due to increased activation of muscles, associated with larger sway amplitude; the stretch reflex torques become smaller due to increased mean absolute velocity of the ankle joint [15], consequently, will have smaller contributions. Finally, the intrinsic stiffness will be smaller due to switch from short range to long range stiffness [32], however, the generated intrinsic torque (which is the multiplication of the stiffness and joint displacement) will be larger due to larger amplitude of joint movement.

The other limitation is the assumption of same EMG-torque TF for TS muscles for central and stretch reflex pathways; in some cases, contribution of some of TS muscles were so small that their EMG-torque relation could not be identified reliably, but collectively, they always produced significant output; thus, we assumed the same EMG-torque relation between them and used weights to account for their contributions.

REFERENCES

[1] R. E. Kearney and I. W. Hunter, "System identification of human joint dynamics," *Critical Rev. Biomed. Eng.*, vol. 18, no. 1, pp. 55–87, 1990.

[2] J. H. Pasma, D. Engelhart, A. C. Schouten, H. van der Kooij, A. B. Maier, and C. G. M. Meskers, "Impaired standing balance: The clinical need for closing the loop," *Neuroscience*, vol. 267, pp. 157–165, May 2014.

[3] T. Kiemel, A. J. Elahi, and J. J. Jeka, "Identification of the plant for upright stance in humans: Multiple movement patterns from a single neural strategy," *J. Neurophysiol.*, vol. 100, no. 6, pp. 3394–3406, Dec. 2008.

[4] T. Sinha and B. E. Maki, "Effect of forward lean on postural ankle dynamics," *IEEE Trans. Rehabil. Eng.*, vol. 4, no. 4, pp. 348–359, Dec. 1996.

[5] R. Fitzpatrick, D. Burke, and S. C. Gandevia, "Loop gain of reflexes controlling human standing measured with the use of postural and vestibular disturbances," *J. Neurophysiol.*, vol. 76, no. 6, pp. 3994–4008, Dec. 1996.

[6] J. H. Pasma, J. van Kordelaar, D. de Kam, V. Weerdesteyn, A. C. Schouten, and H. van der Kooij, "Assessment of the underlying systems involved in standing balance: The additional value of electromyography in system identification and parameter estimation," *J. Neuroeng. Rehabil.*, vol. 14, no. 1, p. 97, Sep. 2017.

[7] C. D. Tokuno, S. J. Garland, M. G. Carpenter, A. Thorstensson, and A. G. Cresswell, "Sway-dependent modulation of the triceps surae H-reflex during standing," *J. Appl. Physiol.*, vol. 104, no. 5, pp. 1359–1365, May 2008.

[8] N. Kawashima, H. Yano, Y. Ohta, and K. Nakazawa, "Stretch reflex modulation during imposed static and dynamic hip movements in standing humans," *Exp. Brain Res.*, vol. 174, no. 2, pp. 342–350, Sep. 2006.

[9] M. M. Mirbagheri, H. Barbeau, and R. E. Kearney, "Intrinsic and reflex contributions to human ankle stiffness: Variation with activation level and position," *Exp. Brain Res.*, vol. 135, no. 4, pp. 423–436, Dec. 2000.

[10] P. Amiri and R. E. Kearney, "Ankle intrinsic stiffness changes with postural sway," *J. Biomech.*, vol. 85, pp. 50–58, Mar. 2019.

[11] P. Amiri, A. Mohebbi, and R. Kearney, "Experimental methods to study human postural control," *J. Visualized Exp.*, vol. 151, Sep. 2019, Art. no. e60078.

[12] P. Amiri, L. J. MacLean, and R. E. Kearney, "Measurement of shank angle during stance using laser range finders," in *Proc. 38th Annu. Int. Conf. IEEE Eng. Med. Biol. Soc. (EMBC)*, Aug. 2016, pp. 3374–3377.

[13] H. J. Hermens, B. Freriks, C. Disselhorst-Klug, and G. Rau, "Development of recommendations for SEMG sensors and sensor placement procedures," *J. Electromyogr. Kinesiol.*, vol. 10, no. 5, pp. 361–74, Oct. 2000, doi: 10.1016/s1050-6411(00)00027-4.

[14] R. E. Kearney, R. B. Stein, and L. Parameswaran, "Identification of intrinsic and reflex contributions to human ankle stiffness dynamics," *IEEE Trans. Biomed. Eng.*, vol. 44, no. 6, pp. 493–504, Jun. 1997.

[15] R. B. Stein and R. E. Kearney, "Nonlinear behavior of muscle reflexes at the human ankle joint," *J. Neurophysiol.*, vol. 73, no. 1, pp. 65–72, Jan. 1995.

[16] R. J. Peterka, "Sensorimotor integration in human postural control," *J. Neurophysiol.*, vol. 88, no. 3, pp. 1097–1118, Sep. 2002.
[17] T. Sinkjaer, E. Toft, K. Larsen, and S. Andreassen, "EMG-torque dynamics at different contraction levels in human ankle muscles," *J. Electromyogr. Kinesiol.*, vol. 3, no. 2, pp. 67–77, Jan. 1993.
[18] W. F. Genadry, R. E. Kearney, and I. W. Hunter, "Dynamic relationship between EMG and torque at the human ankle: Variation with contraction level and modulation," *Med. Biol. Eng. Comput.*, vol. 26, no. 5, pp. 489–496, Sep. 1988.
[19] M. A. Golkar, K. Jalaleddini, and R. E. Kearney, "EMG-torque dynamics change with contraction bandwidth," *IEEE Trans. Neural Syst. Rehabil. Eng.*, vol. 26, no. 4, pp. 807–816, Apr. 2018.
[20] P. Amiri and R. E. Kearney, "A closed-loop method to identify EMG-torque dynamics in human balance control," in *Proc. 41st Annu. Int. Conf. IEEE Eng. Med. Biol. Soc. (EMBC)*, Jul. 2019, pp. 5059–5062.
[21] P. Amiri and R. E. Kearney, "Ankle intrinsic stiffness is modulated by postural sway," in *Proc. 39th Annu. Int. Conf. IEEE Eng. Med. Biol. Soc. (EMBC)*, Jul. 2017, pp. 70–73.
[22] U. Forssell and L. Ljung, "Closed-loop identification revisited," *Automatica*, vol. 35, no. 7, pp. 1215–1241, Jul. 1999.
[23] K. Jalaleddini, E. S. Tehrani, and R. E. Kearney, "A subspace approach to the structural decomposition and identification of ankle joint dynamic stiffness," *IEEE Trans. Biomed. Eng.*, vol. 64, no. 6, pp. 1357–1368, Jun. 2017.
[24] H. Tani and H. Nagasaki, "Contractile properties of human ankle muscles determined by a systems analysis method for the EMG-force relationship," *J. Electromyogr. Kinesiol.*, vol. 6, no. 3, pp. 205–213, Sep. 1996.
[25] W. Yao, R. J. Fuglevand, and R. M. Enoka, "Motor-unit synchronization increases EMG amplitude and decreases force steadiness of simulated contractions," *J. Neurophysiol.*, vol. 83, no. 1, pp. 441–452, Jan. 2000.
[26] N. A. Maffiuletti, P. Aagaard, A. J. Blazevich, J. Folland, N. Tillin, and J. Duchateau, "Rate of force development: Physiological and methodological considerations," *Eur. J. Appl. Physiol.*, vol. 116, no. 6, pp. 1091–1116, Jun. 2016.
[27] E. Toft, T. Sinkjaer, S. Andreassen, and K. Larsen, "Mechanical and electromyographic responses to stretch of the human ankle extensors," *J. Neurophysiol.*, vol. 65, no. 6, pp. 1402–1410, Jun. 1991.
[28] J. H. Pasma, D. Engelhart, A. B. Maier, A. C. Schouten, H. van der Kooij, and C. G. Meskers, "Changes in sensory reweighting of proprioceptive information during standing balance with age and disease," *J. Neurophysiol.*, vol. 114, no. 6, pp. 3220–3233, Dec. 2015.
[29] I. D. Loram and M. Lakie, "Direct measurement of human ankle stiffness during quiet standing: The intrinsic mechanical stiffness is insufficient for stability," *J. Physiol.*, vol. 545, no. 3, pp. 1041–1053, Dec. 2002.
[30] P. J. Bock, R. E. Kearney, S. M. Forster, and R. Wagner, "Modulation of stretch reflex excitability during quiet human standing," in *Proc. 26th Annu. Int. Conf. IEEE Eng. Med. Biol. Soc.*, Sep. 2004, pp. 4684–4687.
[31] P. Amiri and R. E. Kearney, "Patterns of muscle activation and modulation of ankle intrinsic stiffness in different postural operating conditions," *J. Neurophysiol.*, vol. 123, no. 2, pp. 743–754, Feb. 2020.
[32] I. D. Loram, C. N. Maganaris, and M. Lakie, "The passive, human calf muscles in relation to standing: The non-linear decrease from short range to long range stiffness," *J. Physiol.*, vol. 584, no. 2, pp. 661–675, Oct. 2007.